



TOGOMI
Algorithm Theoretical Basis
Document

REF :
TOGOMI/KNMI/ATBD/001
ISSUE : 1.2
DATE : 01-11-2003

DOCUMENT TYPE: ATBD

TITLE:

TOGOMI
Algorithm Theoretical Basis Document

	FUNCTION	NAME	DATE	SIGNATURE
PREPARED BY	Scientist	Pieter Valks	01-11-2003	
CHECKED BY				
APPROVED BY	Project Manager	Roeland van Oss	01-11-2003	

DOCUMENT IDENTIFICATION	WBS Nr	KEYWORDS
-------------------------	--------	----------



TOGOMI
Algorithm Theoretical Basis
Document

REF : TOGOMI/KNMI/ATBD/001
ISSUE : 1.2
DATE : 01-11-2003
PAGE : II

DISTRIBUTION LIST

Nr	Destination



TOGOMI
Algorithm Theoretical Basis
Document

REF : TOGOMI/KNMI/ATBD/001
ISSUE : 1.2
DATE : 01-11-2003
PAGE : III

DOCUMENT STATUS SHEET

Issue	Date	Modified Items / Reason for Change
1.0	25.03.2002	First issue
1.1	11.06.2003	Issue for MTR Added section on validation plans
1.2	01.11.2003	Changed format of document Section 3.3.3: TOMS v8 climatology is used instead of Fortuin-Kelder


	<p style="text-align: center;">TOGOMI Algorithm Theoretical Basis Document</p>	REF : TOGOMI/KNMI/ATBD/001 ISSUE : 1.2 DATE : 01-11-2003 PAGE : IV
---	---	---

TABLE OF CONTENTS


1.	INTRODUCTION	1
1.1	Purpose	1
1.2	Scope 1	
1.3	Glossary	1
1.3.1	Acronyms	1
1.4	References	2
1.4.1	Applicable Documents.....	2
1.4.2	Reference Documents	2
2.	BACKGROUND	6
2.1	Overview	6
2.2	Product description	6
3.	ALGORITHM DESCRIPTION	8
3.1	Improvement of GOME level-1 spectra.....	8
3.2	Slant Column Density.....	9
3.2.1	Basic concept.....	9
3.2.2	Ring effect: Raman scattering	10
3.2.3	Instrumental Errors	11
3.2.4	Ozone absorption cross-section and temperature dependence	12
3.2.5	Fit window	13
3.2.6	Fit Method	14
3.3	Air Mass Factor (AMF).....	14
3.3.1	Computation	15
3.3.2	Radiative transfer model.....	16
3.3.3	Look-up-Table.....	16
3.4	Cloud Correction.....	18
3.4.1	FRESCO cloud algorithm.....	18
3.4.2	Air Mass Factor for Partly Cloudy Conditions	19
3.4.3	Ghost Column	19
3.4.4	Total Vertical Column Density	20
4.	ERROR ANALYSIS	21
4.1	Slant column density	21
4.1.1.1	Forward model errors	21
4.1.1.2	<i>A priori</i> errors	21
4.1.1.3	Instrument errors	22
4.2	Air mass factor (AMF).....	23
4.2.1.1	Forward model errors.....	23
4.2.1.2	<i>A priori</i> errors	23
4.3	Cloud correction	24



TOGOMI
Algorithm Theoretical Basis
Document

REF : TOGOMI/KNMI/ATBD/001
ISSUE : 1.2
DATE : 01-11-2003
PAGE : V

4.4 Error Budget.....	24
4.5 Exceptional Cases.....	26
4.5.1.1 Desert Dust	26
4.5.1.2 Biomass Burning	26
4.5.1.3 Polar Stratospheric Clouds.....	26
4.5.1.4 Large Solar Zenith Angles.....	27
5. VALIDATION.....	28

	TOGOMI Algorithm Theoretical Basis Document	REF : TOGOMI/KNMI/ATBD/001 ISSUE : 1.2 DATE : 01-11-2003 PAGE : 1
---	--	--

1. INTRODUCTION

1.1 Purpose

This document is the Algorithm Theoretical Baseline Document for the GOME Total Ozone retrieval algorithm TOGOMI.


1.2 Scope

This ATBD details the TOGOMI retrieval algorithm used to derive total ozone columns from the GOME level-1 product.

1.3 Glossary

1.3.1 Acronyms

AMF	Air-Mass Factor
ATBD	Algorithm Theoretical Basis Document
B&P	Bass and Paur
DAK	Doubling Adding KNMI
DOAS	Differential Optical Absorption Spectroscopy
DLR	Deutsches Zentrum für Luft- und Raumfahrt
ECMWF	European Centre for Medium-range Weather Forecast
ERS	European Remote Sensing Satellite
ESA	European Space Agency
FM	Flight Model
FRESCO	Fast Retrieval Scheme for Cloud Observables
FWHM	Full Width Half Maximum
GAW	Global Atmospheric Watch
GDP	GOME Data Processor
GOME	Global Ozone Monitoring Instrument
GSAG	GOME Science Advisory Group
KNMI	Royal Netherlands Meteorological Institute
LUT	Look Up Table
OMI	Ozone Monitoring Instrument
PSC	Polar Stratospheric Clouds
RTM	Radiative Transfer Model
SZA	Solar Zenith Angle
TOAR	Top-Of-the-Atmosphere Reflectance
TOGOMI	Total Ozone algorithm for GOME using the OMI algorithm
TOMS	Total Ozone Mapping Spectrometer

	TOGOMI Algorithm Theoretical Basis Document	REF : TOGOMI/KNMI/ATBD/001 ISSUE : 1.2 DATE : 01-11-2003 PAGE : 2
---	--	--

UV	Ultra Violet
VIS	Visible
WMO	World Meteorological Organisation


1.4 References

1.4.1 Applicable Documents

- [AD1] Development of Algorithms for Retrieval of GOME Total Ozone Column, Statement of Work, ERSE-DTEX-EOAD-SW-02-0001, Issue 1, Revision 0, April 2002
- [AD2] ESRIN/Contract No. 16401/02/I-LG, Development of Algorithms for Retrieval of GOME Total Ozone Column

1.4.2 Reference Documents

- [RD1] Bass and Paur. The ultraviolet cross-sections of ozone. I. The measurements. II - Results and temperature dependence, In *Proc. Quadrennial Ozone Symp.*, Chalkidiki, Greece, Eds. C. Zefros and A. Ghazi. Reidel, Dordrecht, 606p., 1986
- [RD2] Burrows, J.P., M. Weber, M. Buchwitz, V. Rozanov, A. Ladstätter-Weissenmayer, A. Richter, R. De Beek, R. Hoogen, K. Bramstedt, K.W. Eichmann, M. Eisinger, and D. Perner, The Global Monitoring Experiment (GOME): Mission concept and first scientific results, *J. Atmos Sci.*, Vol 56, 151-175, 1999a.
- [RD3] Burrows, J.P., Richter, A., Dehn, A., Deters, B., Himmelmann, S., Voigt, S., Orphal, J., Atmospheric remote-sensing reference data from GOME - 2. Temperature-dependent absorption cross sections of O₃ in the 231-794 nm range. *Journal of Quantitative Spectroscopy & Radiative Transfer*, 61, pp. 509-517. 1999b.
- [RD4] Chance, K. and R.J.D. Spurr, Ring Effect Studies: Rayleigh Scattering, Including Molecular Parameters for Rotational Raman Scattering, and the Fraunhofer Spectrum, *Applied Optics* 36, 5224-5230, 1997.
- [RD5] De Haan, J.F., P.B. Bosma, and J.W. Hovenier, The adding method for multiple scattering calculations of polarized light, *Astron. Astrophys. Vol 183*, 371-391, 1987.
- [RD6] De Haan, J.F., Accounting for Raman Scattering in DOAS, *SN-OMIE-KNMI-409*, KNMI, 2003.
- [RD7] De Rooij, W.A., van der Stap, C.C.A.H., 1984, Expansion of Mie Scattering Matrices in Generalized Spherical Functions, *Astron. & Astrophys*, Vol 131, 237-248.
- [RD8] Eskes et al.. A new approach to GOME NO₂. In: *Final report of the project "Sciamachy Data Assimilation"*, Beleidscommissie Remote Sensing (BCRS) project 4.1/AP-09, February 2001.
- [RD9] Fortuin J.P.F., and H. Kelder, An ozone climatology based on ozonesonde and satellite measurements, *J. Geophys. Res.*, Vol 103, NO. D23, 31,709-31,734, 1998.

	TOGOMI Algorithm Theoretical Basis Document	REF : TOGOMI/KNMI/ATBD/001 ISSUE : 1.2 DATE : 01-11-2003 PAGE : 3
---	--	--

- [RD10] Fong, K.W., T.H. Jefferson, T. Suyehiro and L. Walton, Guide to the SLATEC Common Mathematical Library, available at: <http://www.netlib.org/slatec/guide>, 1993.
- [RD11] Koelemeijer, R.B.A., and P. Stammes, Effects of clouds on ozone column retrieval from GOME UV measurements, *J. Geophys. Res.*, 104, NO. D7, 8,281- 8,294, 1999.
- [RD12] Koelemeijer, R.B.A., Effect of Lambert surface approximation for clouds on the air mass factor of ozone in the UV, KNMI memo, March 7, 2001.
- [RD13] Koelemeijer, R.B.A., P. Stammes, J.W. Hovenier, and J.F. de Haan, A fast method for retrieval of cloud parameters using oxygen A-band measurements from GOME, *J. of Geophys. Res.*, 106, 3475-3490, 2001.
- [RD14] Koelemeijer, R.B.A., P. Stammes, J.W. Hovenier, and J.F. de Haan, Global distributions of effective cloud fraction and cloud top pressure derived from oxygen A-band spectra measured by the Global Ozone Monitoring Experiment: comparison to ISCCP data, *J. of Geophys. Res.*, 107, 4151, 2002.
- [RD15] Koelemeijer, R.B.A., J.F. de Haan, and P. Stammes, A database of spectral surface reflectivity in the range 335-772 nm derived from 5.5 years of GOME observations, *J. of Geophys. Res.*, 108, 4070, 2003.
- [RD16] Lambert, J.C., M. van Roozendaal, M. de Maziere, P.C. Simon, J.P. Pommereau, F. Goutail, A. Sarkissian and J.F. Gleason, Investigation of the Pole-to-Pole performance of spaceborne atmospheric chemistry sensors with the NDSC, *J. Atmos. Sci.*, Vol. 56, 176-193, 1999.
- [RD17] Lambert, J.C. (ed), ERS-2 GOME GDP 3.0 Implementation and Delta Validation. Validation Report for GOME Level-1-to-2 Data Processor Upgrade to Version 3.0, ERSE-DTEX OAD-TN-02-0006, Version 1.0, November 2002
- [RD18] Levelt, P.F., and co-authors, Science Requirements Document for OMI-EOS, RS-OMIE-KNMI-001, Version 2, ISBN 90-369-2187-2, 2000.
- [RD19] Martin, R.V., K. Chance, D.J. Jacob, T.P. Kurosu, R.J.D. Spurr, E. Bucsela, J.F. Gleason, P.I. Palmer, I. Bey, A.M. Fiore, Q. Li, R.M. Yantosca, and R.B.A. Koelemeijer, An improved retrieval of tropospheric nitrogen dioxide from GOME, *J. Geophys. Res.*, 107, 4437, 2002b.
- [RD20] Mishchenko, M.I., and L. D. Travis, Capabilities and limitations of a current FORTRAN implementation of the T-matrix method for randomly oriented, rotationally symmetric scatterers, *J. Quant. Spectrosc. Radiat. Transfer*, Vol 60, 309-324, 1998
- [RD21] More, J. J., The Levenberg-Marquardt algorithm: implementation and theory. In Numerical Analysis Proceedings (Dundee, June 28 - July 1, 1977, G. A. Watson, Editor), *Lecture Notes in Mathematics 630*, Springer-Verlag, 1978.
- [RD22] Orphal, J., A critical review of the absorption cross-sections of O₃ and NO₂ in the 240-790 nm region, ESA Technical Note MO-TN-ESA-GO-0302, 2002.
- [RD23] Schutgens N.A.J., and P. Stammes, Parametrisation of Earth's polarisation spectrum from 290 to 330 nm, *J. Quantitative Spectroscopy and Radiative Transfer*, 239-255, 2002.
-



TOGOMI
Algorithm Theoretical Basis
Document


REF : TOGOMI/KNMI/ATBD/001
ISSUE : 1.2
DATE : 01-11-2003
PAGE : 4

- [RD24] Spurr, R., W. Thomas and D. Loyola, GOME Level 1 to 2 Algorithms Description, DLR Technical note ER-TN-DLR-GO-0025, Rev. 3/A, Oberpfaffenhofen, Germany, 2002.
- [RD25] Stammes, P., J.F. de Haan, and J.W. Hovenier, The polarized internal radiation field of a planetary atmosphere, *Astron. Astrophys. Vol 225*, 239-259, 1989
- [RD26] Stammes, P., Spectral radiance modelling in the UV-Visible range, to appear in: *IRS 2000: Current problems in Atmospheric Radiation*, Eds. W.L. Smith and Y.M. Timofeyev, A. Deepak Publ., Hampton (VA), 2001.
- [RD27] Van der A, R., Recalibration of GOME spectra for the purpose of ozone profile retrieval, *Technical Report TR-236*, KNMI, De Bilt, The Netherlands, 2001.
- [RD28] Van de Hulst, H.C., Multiple Light Scattering. Tables, Formulas and Applications. Academic Press, San Diego, Ca., pp 573-577, 1980.
- [RD29] Van Geffen, J.H.G.M., Documentation of the software package GomeCal (version 1.0), *Technical report TR-255*, KNMI, De Bilt, The Netherlands, 2003a.
- [RD30] Van Geffen, J.H.G.M. and R.F. Van Oss, Wavelength calibration of spectra measured by GOME using a high-resolution reference spectrum, *Applied Optics*, 42, 2739-2753, 2003b.
- [RD31] Van Roozendael, V. Soebijanta, C.Fayt, and J.-C. Lambert, Investigation of DOAS issues affecting the accuracy of the GDP version 3.0 total ozone product, in *ERS-2 GOME GDP 3.0 Implementation and Delta Validation Report*. Issue 1.0, 2002.
- [RD32] Veefkind, J.P., Temperature effects on ozone slant column density, draft 2, *Tech. Rep.*, TN-OMIE-KNMI-234, KNMI, De Bilt, The Netherlands, 2000a.
- [RD33] Veefkind, J.P., Effects of instrument signal-to-noise on ozone DOAS, *Tech. Rep.*, TN-OMIE-KNMI-239, KNMI, De Bilt, The Netherlands, 2000b.
- [RD34] Veefkind, J.P., Effect of ozone profile shape on the slant column density, *Tech. Rep.*, TN-OMIE-KNMI-232, KNMI, De Bilt, The Netherlands, 2000c.
- [RD35] Veefkind, J.P. and J.F. de Haan, OMI Algorithm Theoretical Basis Document, Barthia, P.K (ed), Volume II - Chapter 3, DOAS Total Ozone Algorithm, *ATBD-OMI-02*, Version 1.0, September 2001.
- [RD36] Veefkind, J.P., Effects of polar stratospheric clouds on the retrieval of OMI DOAS total ozone, *Tech. Rep*, SN-OMIE-KNMI-321, KNMI, De Bilt, The Netherlands, 2002.
- [RD37] Vountas, M., Rozanov, V.V., and Burrows, J.P. 1997. Ring Effect: Impact of rotational Raman scattering on radiative transfer in Earth's Atmosphere, *Journal of Quantitative Spectroscopy and Radiative Transfer*, Vol. 60, No. 6, 943-961, 1998.
- [RD38] WMO, WMO Scientific Assessment of Ozone Depletion: 1998, *WMO-GAW report*, 1999.
- [RD39] WMO, WMO Scientific Assessment of Ozone Depletion: 2002, *WMO-GAW report*, 2003.
-



TOGOMI
Algorithm Theoretical Basis
Document

REF : TOGOMI/KNMI/ATBD/001
ISSUE : 1.2
DATE : 01-11-2003
PAGE : 5

	TOGOMI Algorithm Theoretical Basis Document	REF : TOGOMI/KNMI/ATBD/001 ISSUE : 1.2 DATE : 01-11-2003 PAGE : 6
---	--	--

2. BACKGROUND

2.1 Overview

The current operational GOME total ozone algorithm (GDP) has been developed by DLR (under ESA responsibility) and is based on the Differential Optical Absorption Spectroscopy (DOAS) method [*Spurr et al.*, 2002; *Burrows et al.*, 1999a] that has been widely used to measure trace gases from ground. The GOME-DOAS algorithm consists of three steps. First, the reference differential absorption spectrum of ozone is fitted to the measured Earth radiance spectrum and solar irradiance spectrum, to obtain the slant column density. In the second step the slant column density is translated into the vertical column density using the so-called air mass factor (AMF). The third step consists of a correction for the screening of ozone below clouds.

The accuracy of the GOME ozone columns of the latest GDP version 3 is significantly improved compared to the previous version. However, preliminary geophysical validation results indicate that a solar zenith angle and seasonal dependent error persists. Since the current DOAS approach in the GDP might not lead to further major improvements, a new improved GOME total ozone retrieval algorithm is necessary.

The new GOME algorithm TOGOMI is based on the total ozone DOAS algorithm developed for the OMI instrument. This resolves various limitations of the current operational GOME algorithm (GDP v3). With respect to total ozone column retrieval using the DOAS method, the OMI and GOME instruments are very similar. Therefore, an adaptation of the OMI total ozone algorithm to the GOME instrument is very well possible. The main improvements of the new algorithm are: (i) treatment of the atmospheric temperature sensitivity by using effective ozone cross-sections calculated from ECMWF temperature profiles, and by selecting a narrow spectral fit window to reduce the temperature sensitivity, (ii) improvements in the calculation of the air mass factor, using the so-called empirical approach and (iii) using the Fast Retrieval Scheme for Clouds from the Oxygen A-band (FRESCO) algorithm for the cloud correction. Improvements in the total ozone product are also achieved by improving the GOME level-1 product (the Earth radiance and solar irradiance spectra) with the GomeCal program [*Van Geffen et al.*, 2003a].

The estimated accuracy of the total column ozone is 2-3%. For the slant column density the expected accuracy is better than 2%. The new GOME total ozone columns will be validated against co-located ground based measurements and compared with the GDP V3 ozone columns and TOMS total ozone measurements.

2.2 Product description

The TOGOMI total ozone product is derived from the GOME level 1 data as produced by the GDP. To improve the wavelength calibration and polarisation correction of the level-1 spectra and to correct for the degradation of the GOME instrument, the GomeCal program is applied to the GDP-level-1 files. This is described in Section 3.1.




TOGOMI
Algorithm Theoretical Basis
Document

REF : TOGOMI/KNMI/ATBD/001
ISSUE : 1.2
DATE : 01-11-2003
PAGE : 7

The main products of the new GOME total ozone algorithm are the ozone vertical column density and the ozone slant column density. The vertical column density is the amount of ozone along a vertical path from the ground to the top-of-the-atmosphere. The slant column density is the amount of ozone along an average path that the photons travel from the Sun through the atmosphere to the satellite sensor. The slant column density concept is described in more detail in Section 3.2. Compared to the vertical column density, very little a priori information is needed to derive the slant column density. As it is a concise representation of the measured radiance spectrum, people from the data assimilation community have expressed a need for the slant column density [Eskes *et al.*, 2001].

The ozone vertical column product should meet the accuracy requirements for ozone trend analyses: satellite instruments should be able to detect a change of 1% in the ozone column over a period of 10 years [WMO, 1999, 2003]. This means that a (relative) accuracy of the ozone vertical column density of 2% is desired [Levelt, 2000]. As the slant column density is one of the parts needed to derive the vertical column density, the accuracy of the slant column density needs to be higher than that for the vertical column density.

	TOGOMI Algorithm Theoretical Basis Document	REF : TOGOMI/KNMI/ATBD/001 ISSUE : 1.2 DATE : 01-11-2003 PAGE : 8
---	--	--

3. ALGORITHM DESCRIPTION

The TOGOMI total ozone algorithm consists of four steps. First, the GomeCal package is applied to the GDP-level-1 files to improve the accuracy of the measured Earth radiance and solar irradiance spectrum. In the second step, the DOAS method is used to fit the reference differential absorption spectrum of ozone to the measured Earth radiance spectrum and solar irradiance spectrum, to obtain the slant column density. In the third step the slant column density is translated into the vertical column density using the so-called air mass factor (AMF). The fourth step consists of a correction for cloud effects. In this section we describe each of these retrieval steps, including the physical background, as well as assumptions and *a priori* information used.


3.1 Improvement of GOME level-1 spectra

The input for the new TOGOMI algorithm is based on the GOME level-1 product as produced by the GDP, but with several improvements. To improve the wavelength calibration of the Earth radiance and solar irradiance spectra, the GomeCal package is applied to the GDP level-1 files [Van Geffen, 2003a]. In addition to a wavelength recalibration, GomeCal applies an improved polarisation correction to the GDP level-1 spectra and a radiometric correction, which includes a correction for the degradation of the GOME instrument.

The standard wavelength calibration of the GDP uses spectral lines of an onboard PrCr/Ne hollow cathode lamp to correct for shifts in the wavelengths associated with the detector pixels, for example caused by temperature effects, with respect to a pre-flight calibration. This calibration is not accurate enough for the retrieval of the DOAS total ozone product. A new calibration method, developed by Van Geffen [2003b], uses as reference spectrum a high-resolution solar spectrum, with irradiance values given at 0.01 nm intervals.

To be able to fit the observations with this reference spectrum, i.e. with the Fraunhofer lines in the solar spectrum, the reference spectrum is convolved with the GOME slit function and subsequently integrated over the spectral bins of the detector. The location and width of these bins are allowed to vary along the detector: both a shift and a squeeze are applied to the measurements (the GDP calibration method with the lamp lines applies only a shift), where the GDP's wavelength grid serves as the initial guess. The improved wavelength grid is found with a tailor-made chi-square minimisation. The method provides a calibration accuracy of 0.001 nm or better above 290 nm, corresponding to about 1/100th of a pixel for the DOAS fitting window. The calibration can be applied to a user specified wavelength window, thus optimising the calibration for subsequent retrieval purposes.

When extracting the GDP level-1 spectra, a polarisation correction can be applied, based on a theoretical value at 300 nm (UV) and polarisation measurements in 100 nm wide windows around 350, 500 and 700 nm. This correction, however, appears to be insufficient, in particular in the UV range. *Schutgens and Stammes* [2002] developed an improved polarisation correction which replaces the GDP's correction. The new polarisation correction is based on a parametrisation of the UV Earthshine polarisation

	TOGOMI Algorithm Theoretical Basis Document	REF : TOGOMI/KNMI/ATBD/001 ISSUE : 1.2 DATE : 01-11-2003 PAGE : 9
---	--	--

between 290 and 330 nm, as function of solar zenith angle, viewing geometry, scene albedo and total ozone column. For wavelengths above 330 nm the method supplies the same polarisation correction as the GDP.

The calibration of the absolute (ir)radiance in the GDP level-1 spectra appears to be insufficiently accurate. Additionally, it has been observed that the GOME instrument shows a degradation, notably since 1998. This degradation is time and wavelength dependent, and the measured earthshine radiances degrade differently from the solar irradiance spectra. The degradation is only partly corrected for when extracting GDP level-1 spectra. In the GOME instrument, Peltier elements are used for cooling the detector. There is some interference of the Peltier cooler conduct signals on the detector signals, for which a correction is included in the standard calibration of the GDP, but this correction does not remove all interference effects.

For these reasons, a radiometric correction procedure was made by *Van der A* [2001] consisting of three parts which can be applied independently, in addition to the corrections of the GDP extractor:

- a radiometric calibration
- a correction for the degradation of the instrument
- a correction to remove residual effects of the interference of the Peltier cooler signals

The first two corrections apply to wavelengths between 265 and 390 nm and correction data are available up to 1 July 2001; for dates after that, the correction of 1 July 2001 is used (the lack of good measured solar spectra severely hinders determining correction data after 1 July 2001).

3.2 Slant Column Density

The first step in the ozone DOAS algorithm is to determine the slant column density. The slant column density is the amount of ozone along an average path that the photons travel from the Sun, through the atmosphere, to the satellite sensor. The slant column density is determined by fitting an analytical function to the measured Earth radiance and solar irradiance data. This fit is applied to data taken in a certain wavelength range, called the fit window. A polynomial function, which serves as a high-pass filter, is applied to account for scattering and absorption that vary gradually with the wavelength, e.g., scattering by molecules, aerosols, and clouds. The slant column density is derived from the filtered data, which contains spectral features of ozone in the fit window. Figure 3.1 shows a DOAS fit applied to GOME level-1 data.

3.2.1 Basic concept

A nadir-viewing instrument like GOME measures the radiance reflected by the Earth and the atmosphere. For spectral ranges where ozone causes the dominant spectral absorption features, the top-of-the-atmosphere reflectance (TOAR) can be approximated by:

$$\rho(\lambda, \theta_0, \theta, \varphi - \varphi_0) = \frac{\pi I}{F_0} = P(\lambda) e^{-\sigma_{O_3}(\lambda) N_s} \quad [3-1]$$

where, ρ is the top-of-the-atmosphere reflectance, I is the Earth radiance, λ is the wavelength, θ_0 is the solar zenith angle; θ is the viewing zenith angle; $\varphi - \varphi_0$ is the relative Sun-satellite azimuth angle; $F_0(\lambda)$ is the extraterrestrial solar irradiance per unit area of the atmosphere, $\sigma_{O_3}(\lambda)$ is the ozone absorption cross section, N_s the ozone slant column density and $P(\lambda)$ is a low order polynomial that acts as high-pass filter.

Equation [3-1] holds for optically thin absorbers and is inspired by the well-known Lambert-Beer law and photon path distributions [Van de Hulst, 1980]. Numerical experiments using radiative transfer calculations (excluding Raman scattering, see next Section) have shown that for ozone absorption in the Earth atmosphere, equation [3-1] is an accurate approximation for wavelengths longer than approximately 320 nm.

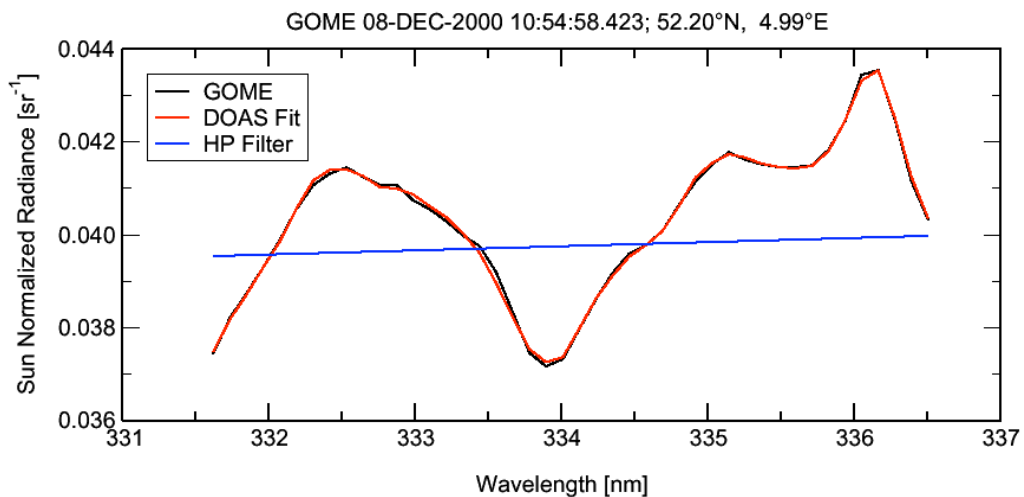



Figure 3.1. DOAS fit applied to GOME data measured over western Europe on December 8, 2000. The spectral resolution of the GOME data was decreased by a low pass filter to avoid undersampling. The black line shows the Sun normalized radiance measured by GOME, the red line shows the DOAS fit of the measured data. The blue line shows the high-pass filter that was used in the fit.

3.2.2 Ring effect: Raman scattering

One of the assumptions underlying Equation [3-1] is that scattering on air molecules is elastic. This is, however, not completely true. About 4% of all scattering events on air molecules is inelastic, resulting in a shift in the photon wavelength up to 2 nm. The most pronounced consequence on the diffuse radiation field is that the solar Fraunhofer lines

	TOGOMI Algorithm Theoretical Basis Document	REF : TOGOMI/KNMI/ATBD/001 ISSUE : 1.2 DATE : 01-11-2003 PAGE : 11
---	--	---

are smeared-out. However, the atmospheric absorption structures are influenced as well, resulting in more-shallow line depths. This has an immediate effect on DOAS trace gas retrievals in case Raman scattering is not taken into account, leading to too-small columns. This error amounts to several percent, motivating a proper treatment of this effect.

We follow the approach introduced by *de Haan* [2003] to deal with Raman scattering in the ozone column retrieval. Equation [3-1] is adjusted to account for Raman scattering by adding a term corresponding to inelastic scattered radiation:

$$\frac{I_{\text{det}}^{\text{meas}}(\lambda)}{F_0^{\text{meas}}(\lambda)} = P_{\text{el}}(\lambda) \left(\exp[-N_s \sigma_x^{\text{el}}(\lambda)] + \frac{P_{\text{inel}}(\lambda)}{P_{\text{el}}(\lambda)} \frac{I_{\text{Ring}}^{\text{eff}}(\lambda)}{F_0^{\text{meas}}(\lambda)} \exp[-N_s \Delta\sigma_x^{\text{eff}}(\lambda)] \right) \quad [3-2]$$

Here, $P_{\text{el}}(\lambda)$ and $P_{\text{inel}}(\lambda)$ are low degree polynomials of the wavelength, representing the overall wavelength dependence due to scattering, $\sigma_x^{\text{el}}(\lambda)$ is the effective absorption cross section of the trace gas for elastic scattering, $I_{\text{Ring}}^{\text{eff}}(\lambda)$ is the commonly used Ring spectrum due to Fraunhofer lines in the solar irradiance. Furthermore,


$$\Delta\sigma_x^{\text{eff}}(\lambda) = (\mu_0 \sigma_x^{\text{ns}}(\lambda) + \mu \sigma_x^{\text{s}}(\lambda)) / (\mu + \mu_0), \quad [3-3]$$

with $\sigma_x^{\text{s}}(\lambda)$ and $\sigma_x^{\text{ns}}(\lambda)$ effective cross sections involving high-resolution solar spectrum and the Raman spectrum, see *de Haan* [2003] for further details; μ_0 is the cosine of the solar zenith angle and μ is the cosine of the viewing angle. Equation [3-2] has been derived starting with two simplifications: (i) the absorber is situated complete above the scattering layer, and (ii), observed radiation is scattered only once (elastic or inelastic). In this situation an algebraic solution for the radiance can be found. Both simplifications are then subsequently left and the resulting implications for the solution are carefully evaluated.

3.2.3 Instrumental Errors

The TOGOMI algorithm uses corrected GDP level 1-data of the backscattered Earth radiance and the solar irradiance as input (see section 3.1). These data contains random and systematic errors. However, DOAS is not affected by systematic errors unless they produce structures that are correlated with ozone absorption spectrum.

For GOME, most of the optical path is the same for the Earth radiance and solar irradiance measurements. Dividing the measured Earth radiance by the measured solar irradiance will lead to a cancellation of errors due to components that are in the optical paths of both the radiance and irradiance measurement. The radiometric accuracy of the TOAR is therefore higher than for the separate radiance or irradiance measurement [*Levelt et. al*, 2000].

	TOGOMI Algorithm Theoretical Basis Document	REF : TOGOMI/KNMI/ATBD/001 ISSUE : 1.2 DATE : 01-11-2003 PAGE : 12
---	--	---

The DOAS method is insensitive to radiometric calibration errors that are multiplicative and constant with wavelength. However, the method is sensitive to additive radiometric errors (offsets). Offsets in the Earth radiance can be accounted for by adding a fit parameter c_a ¹:

$$\rho(\lambda, \theta_0, \theta, \varphi - \varphi_0) = \{RHS Eq.[3.2]\} + c_a / F_0(\lambda). \quad [3-4]$$

Note that in the last term of equation [3-4] $F_0(\lambda)$ is the solar irradiance measured by GOME.


If the GOME radiance or irradiance data show radiometric errors with spectral structure in the DOAS fit window, it depends on the spectral features whether a correction can be made. If the spectral feature is weak, well characterized and doesn't interfere with the ozone absorption cross section, it may be possible to account for it in the fit. In this case, the spectral structure of the error is fitted in the DOAS equation using an extra fitting parameter. Errors that interfere with the ozone absorption cross section cannot be corrected for. If this happens, another fit window should be used that does not show such an interference.

3.2.4 Ozone absorption cross-section and temperature dependence

The accuracy of the slant column retrieval depends on the accuracy and suitability of the laboratory absorption cross-section data used in the DOAS fit. Ozone absorption cross-sections have been measured as a function of wavelength and temperature. For the TOGOMI algorithm, two well-established data sets of ozone absorption cross-sections are considered: the GOME Flight Model (FM98) and Bass and Paur (B&P) cross-sections. The FM98 cross-sections have been measured at 5 different temperatures during the pre-flight calibration using the GOME flight model [Burrows *et al.*, 1999b]. The B&P cross-sections [Bass and Paur, 1986] have been measured at high resolution (better than 0.025nm) and have been recently recommended as a standard for use in remote-sensing applications [Orphal, 2002].

The study of the accuracy of GDP v3 total ozone product by Van Roozendaal *et al.*, [2002] shows the importance of the cross-section quality and the treatment of the temperature dependence in the DOAS fit. This study indicates that the use of FM98 cross-sections results in a high quality and stable DOAS fit when applying a fixed shift of +0.017 nm to the cross-sections. To account for the temperature dependence, an effective ozone absorption cross-section is calculated using daily temperature analyses (or forecast) from the European Centre for Medium-Range Weather Forecasts (ECMWF) model:

¹ The behavior of the fit parameter c_a over the lifetime of GOME, may be used to monitor the long term stability of the instrument. It is not possible to add a fit parameter to account for offsets in the measured solar irradiance, because this results in an unstable fit. However, the solar irradiance is well known and the expected offset in the solar irradiance measurements is small

	TOGOMI Algorithm Theoretical Basis Document	REF : TOGOMI/KNMI/ATBD/001 ISSUE : 1.2 DATE : 01-11-2003 PAGE : 13
---	--	---

$$\sigma_{o_3,eff}(\lambda) = \frac{\int \rho(z) \sigma_{o_3}(T(z), \lambda) dz}{\int \rho(z) dz} \quad [3-5]$$

where $\rho(z)$ is the ozone concentration at altitude z , here determined from the ozone profile climatology from Logan, Labow & McPeters, as used in the TOMS v8 total ozone algorithm, and $\int \rho(z) dz$ is the corresponding vertical ozone column. $T(z)$ is the ECMWF temperature at altitude z (the new ECMWF model provides temperatures for 60 vertical levels), and $\sigma_{o_3}(T(z), \lambda)$ is the temperature dependent ozone absorption cross-section. The resulting effective cross-section $\sigma_{o_3,eff}$ is used in equation [3-4] to calculate the ozone slant column density.

To avoid problems due to the uncertainty in the GOME slit function and the GOME undersampling, the effective spectral resolution of the GOME spectra and the cross-sections is reduced by applying a low pass filter. An advantage of this procedure is that the effective slit function is known very accurately, as it is determined by the low pass filtering. For ozone retrieval in the Huggins band, an effective slit function with a FWHM up to 0.6 nm can be used [Burrows *et al.*, 2002].


3.2.5 Fit window

In this section we describe the fit window choice for the TOGOMI algorithm. Detailed studies were performed to select suitable fit windows for ozone with respect to the following [Veeffkind, 2000a,b,c]:

- Temperature profile
- Instrument signal-to-noise
- Ozone profile
- Other trace gases
- Ring effect.

The conclusions of these studies are that the main drivers for the fit window choice are the sensitivity of the slant column density to atmospheric temperature and to instrument signal-to-noise. The temperature sensitivity is small for narrow fit windows in distinct wavelength regions. On the other hand, the effect of signal-to-noise is less for wider fit windows. The current GOME ozone fitting window, as used in the GDP v3, is 10 nm wide, centered around 330 nm. This is a temperature sensitive fit window with a high s/n ratio. In the TOGOMI algorithm, the temperature sensitivity is taken into account by using an effective ozone cross-section, as described in the previous section.

A good compromise between temperature dependence and signal-to-noise was found to be a 5 nm wide window centered around 334.1 nm. Although the differential absorption of ozone is smaller compared to the current GOME window, the effects of the instrument signal-to-noise on the slant column density are still below ~1.5% [Veeffkind, 2000b]. Both the wide and narrow fit windows will be implemented in the TOGOMI algorithm.

	TOGOMI Algorithm Theoretical Basis Document	REF : TOGOMI/KNMI/ATBD/001 ISSUE : 1.2 DATE : 01-11-2003 PAGE : 14
---	--	---

3.2.6 Fit Method

The slant column density is determined by fitting equation [3-4] to the measured TOAR for the fit window. As described in Section 3.2.4, first the effective spectral resolution of the TOAR and the cross-sections is reduced by applying a low pass filter. Then, the fit is performed using a least squares fitting procedure, which minimizes the merit function given by:

$$\chi^2 = \sum_{i=1}^N \left(\frac{y_{meas}(\lambda_i) - y_{sim}(\lambda_i)}{\varepsilon_{meas}(\lambda_i)} \right)^2, \quad [3-6]$$

where, $y_{meas}(\lambda_i)$ is the measured TOAR, $y_{sim}(\lambda_i)$ is the simulated TOAR radiance as given by Eq. [3-4] and $\varepsilon_{meas}(\lambda_i)$ is the precision of the measured TOAR. The fit window is between λ_1 and λ_N .

The simulated TOAR (Eq. [3-4]) is a non-linear function of the fit parameters. Therefore, a non-linear fit routine should be applied. A modified Levenberg-Marquardt method [More, 1978], as adapted from the SLATEC mathematical library [Fong *et al.*, 1993], is used for the non-linear fitting. Information on the quality of the fit is derived from the covariance matrix. The variance of the fitted parameters, as well as the correlation between them, is also obtained from the covariance matrix.

3.3 Air Mass Factor (AMF)


In the ozone DOAS algorithm, the air mass factor is used to translate the slant column density into a vertical column density. The air mass factor M is defined as the ratio of the slant column density, N_s , and the vertical column density, N_v , i.e.,

$$M \equiv \frac{N_s}{N_v} \quad [3-7]$$

The DOAS fit results in one slant column density for the entire fit window. From the definition of the AMF (Eq. [3-7]), it is clear that there is also one AMF for a fit window.

The AMF depends on the Sun-satellite geometry, as well on the “state of the atmosphere”. With the latter it is meant that AMF depends on the ozone profile, on clouds and aerosol properties, on surface reflectivity properties, etc. Often, the AMF will vary approximately as the geometrical AMF, $M_g = \sec(\theta) + \sec(\theta_0)$. To eliminate most of the geometrical effects, it is convenient to introduce an effective AMF, M_e , defined as

$$M_e = \frac{M}{M_g}. \quad [3-8]$$

	TOGOMI Algorithm Theoretical Basis Document	REF : TOGOMI/KNMI/ATBD/001 ISSUE : 1.2 DATE : 01-11-2003 PAGE : 15
---	--	---

3.3.1 Computation

The AMF can be determined using a radiative transfer model and a GOME simulator. The radiative transfer model produces radiances for a model atmosphere. The GOME simulator is used to produce spectra with the resolution and sampling of GOME. We determine the slant column density by fitting DOAS to these spectra and divide by the known vertical column density to determine the airmass factor. The advantage of this procedure is that exactly the same DOAS fit is applied to the synthetic GOME spectra and to the measured GOME spectra. If the model atmosphere is representative of the ‘real’ atmosphere, this may lead to a cancellation of certain errors.

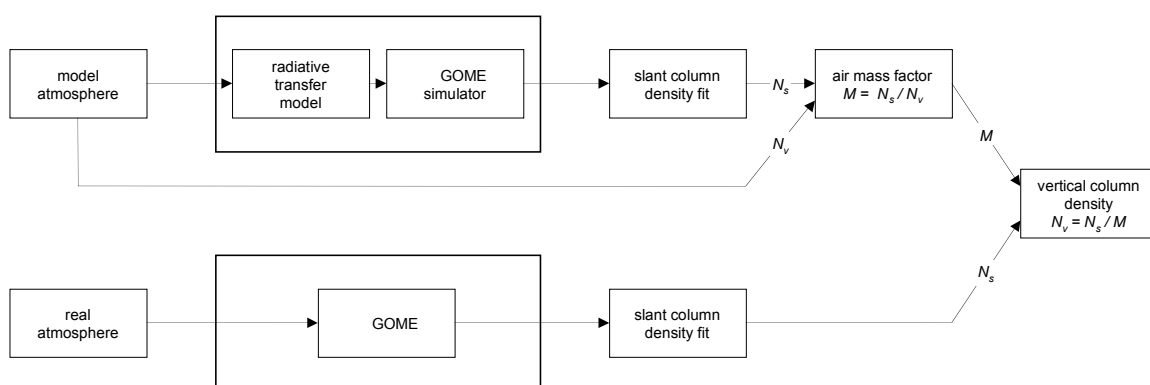



Figure 3.2 Schematic of the empirical DOAS method for GOME.

The AMF depends, among other parameters, on the ozone profile. The ozone profiles in the atmosphere vary strongly, resulting in changes of several percent in the effective air mass factor, depending on the Sun-satellite geometry. To reduce the uncertainty in the AMF due to the ozone profile, a slant column density dependent AMF is used. To derive a relation between the slant column density and the AMF, a set of ozone profiles is used that cover the natural variability of the ozone profile for a given location and time period. For each of these profiles the AMF is calculated for a given Sun/satellite geometry and surface properties. This procedure is illustrated in Figure 3.3. The top panel shows a set of ozone profiles that are representative for 55°N for December. These profiles are taken from the ozone profile climatology from Logan, Labow & McPeters as used in the TOMS V8 total ozone algorithm. This climatology contains 3 (at low-latitudes) to 10 (at high-latitudes) column classified ozone profiles per 10° latitude band for each month. The bottom panel of Figure 3.3 shows the effective AMF for each of the profiles, plotted as a function of slant column density. As can be seen in Figure 3.3, the effective AMF varies almost linearly with the slant column density. This is used in the TOGOMI algorithm, by making the effective AMF a linear function of the slant column density determined in the DOAS fit, as indicated in the bottom panel. This method thus reduces the uncertainty in the AMF due to ozone profile changes with respect to the climatology. The algorithm uses a look-up-table (LUT) of effective AMFs. By using a look-up-table, no radiative transfer calculations have to be done on-line, which results in better performance.

	TOGOMI Algorithm Theoretical Basis Document	REF : TOGOMI/KNMI/ATBD/001 ISSUE : 1.2 DATE : 01-11-2003 PAGE : 16
---	--	---

3.3.2 Radiative transfer model

The radiative transfer model used for the simulations of spectra and, consequently, for the calculation of the AMFs (see Fig. 3.2) is the Doubling-Adding-KNMI (DAK) model [De Haan *et al.*, 1987; Stammes *et al.*, 1989; and Stammes *et al.*, 2000]. Single scattering properties of aerosol particles and PSCs are calculated with a Mie scattering code [De Rooij and Van der Stap, 1984] that generates coefficients for the expansion in generalized spherical functions. These functions can directly be read by the DAK code making efficient calculations for polarized light possible. Note that the T-matrix code for non-spherical particles of Mishchenko produces similar output in terms of generalized spherical functions, which makes calculations for non-spherical particles straightforward (see e.g. Mishchenko and Travis [1998]). The code has the advantage that it is fast for cloudy atmospheres, is well suited for polarized radiative transfer calculations and is very accurate for relatively simple atmospheric models such as homogeneous cloud layers. Recently, the DAK model has been extended so that a (quasi) spherical geometry can be used. Note that a change in code will only affect the look up tables and does not change the algorithm itself, which means that the code can be replaced at a relatively late moment.

3.3.3 Look-up-Table

The look-up-table contains the effective AMFs as function of Sun-satellite geometry, surface reflectivity, surface pressures and ozone profile. As mentioned above, the ozone profiles are taken from the Logan, Labow & McPeters climatology. Besides ozone, molecular scattering and absorption by NO₂ and BrO are accounted for in the radiative transfer calculations. Clouds are represented by Lambertian surfaces with an albedo 0.8, as recommended by Koelemeijer and Stammes [1999] (see also section 3.4).

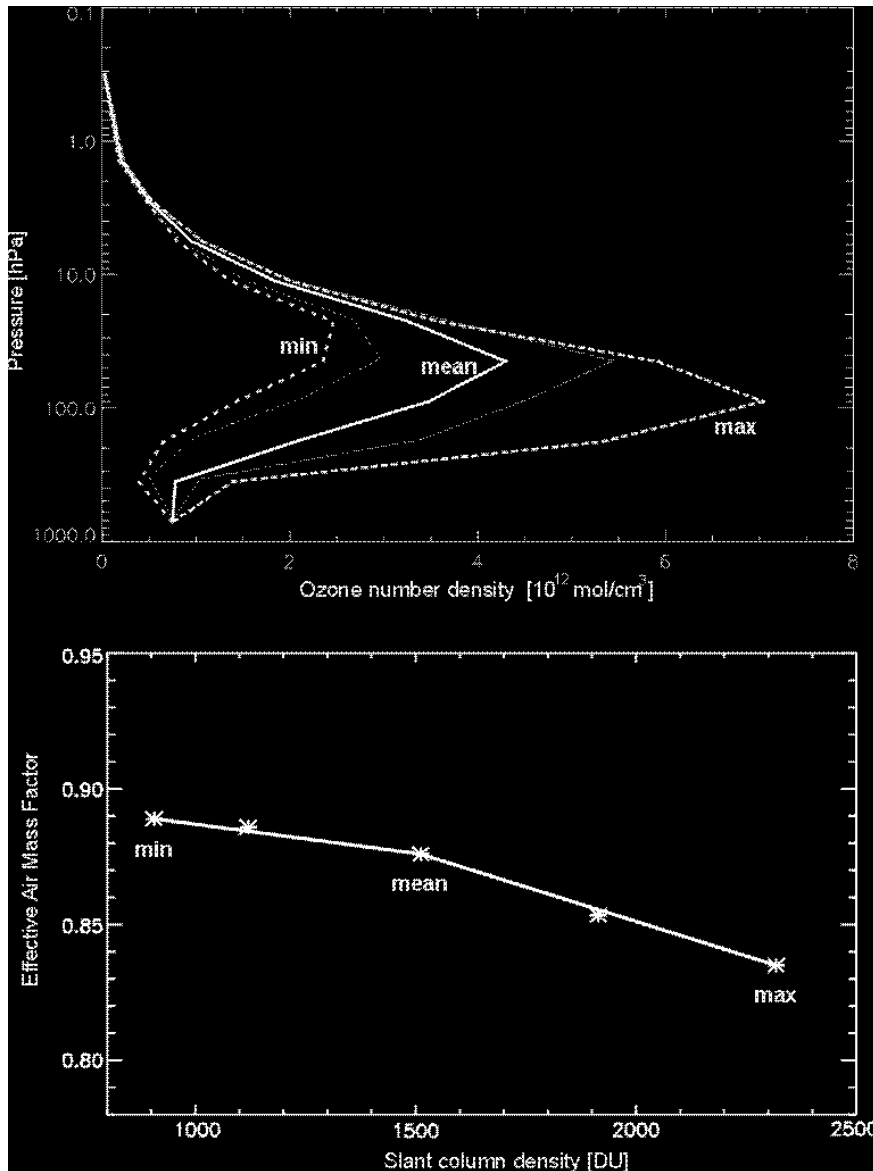


Figure 3.3. Top panel: Five ozone profiles from the Logan, Labow & McPeters climatology [see Bhartia and Wellemeyer, 2002] for 55°N for December. The thick lines denote the ozone profiles with the smallest vertical columns density ($N_v=225$ DU), an average ozone profile ($N_v=375$ DU), and the ozone profile with the largest vertical columns density ($N_v=575$ DU). Two additional ozone profiles with $N_v=275$ DU and $N_v=475$ DU are also plotted. Bottom panel: Effective AMF computed for the five ozone profiles shown in the top panel, plotted as a function of the slant column density. The effective AMFs have been calculated for a solar zenith angle of 75° and a surface albedo of 0.05, using the 325-335 nm DOAS fit-window.


	TOGOMI Algorithm Theoretical Basis Document	REF : TOGOMI/KNMI/ATBD/001 ISSUE : 1.2 DATE : 01-11-2003 PAGE : 18
---	--	---

Table 3.1. Specification of the air mass factor look-up-table dimensions.

Dimension name	Min. value	Max. value	Number of entries
Solar zenith angle	0°	89.25°	11
Viewing zenith angle	0°	89.25°	11
Relative azimuth angle	0°	180°	7
Surface reflectivity	0	1.0	5
Surface pressure	126 hPa	1013 hPa	4
Latitude	-90°	+90°	18
Month	1	12	12
Ozone profile	na	na	3


The AMF is obtained by interpolation in the look-up table. In Table 3.1 the dimensions of the look-up table are presented, as well as the foreseen number of entries for each dimension. The inputs that are needed for the interpolation in this look-up table are taken from the following sources. The solar and viewing zenith angles are taken from the GOME level-1 data. The surface reflectivity is determined from a monthly climatology determined by GOME [Koelemeijer *et al.*, 2003]. The surface pressure will be determined from the terrain height, as contained in the level-1 data. The AMF look-up tables will also be interpolated to the latitude and the date of the measurement. Interpolation between the mean and perturbed ozone profiles is done using the method outlined above, using the slant column density as input.

3.4 Cloud Correction

In case of a cloudy or partly cloudy pixel, part of the ozone column is covered by clouds. Therefore, a cloud correction is needed, which is described in this section. First we describe the FRESCO cloud algorithm, then the computation of the AMF for a partly cloudy pixel, followed by a description of the correction for the so-called ghost column. Finally, we discuss the computation of the total vertical column density.

3.4.1 FRESCO cloud algorithm

To determine the AMF for cloudy conditions, the cloud fraction and cloud pressure are needed, which are derived with the Fast Retrieval Scheme for Clouds from the Oxygen A-band (FRESCO) method [Koelemeijer *et al.*, 2001, 2002]. The retrieval is based on a non-linear least squares fitting of the reflectivity spectrum measured by GOME to a simulated spectrum in the range 758-766 nm, and solving for cloud fraction and cloud top pressure. The cloud model represents clouds by Lambertian surfaces or with a BRDF based on Doubling-Adding and Mie calculations. The cloud fraction is derived assuming a cloud albedo of 0.8, corresponding to an optically thick cloud, and this should therefore be regarded as an effective cloud fraction. This cloud albedo choice has been optimised for ozone air mass factor calculations in the UV, when a ghost-column is added to the derived vertical column density to correct for ozone below the cloud, as described below.

	TOGOMI Algorithm Theoretical Basis Document	REF : TOGOMI/KNMI/ATBD/001 ISSUE : 1.2 DATE : 01-11-2003 PAGE : 19
---	--	---

In the FRESCO method, it is assumed that the absorption below the cloud may be neglected, which can be justified for optically thick clouds. Choosing a high cloud albedo of 0.8 ensures that the model assumptions are internally consistent. The cloud top pressure is derived from the depth of the oxygen A-band, which depends on the absorption optical thickness above the cloud.

This FRESCO cloud model considers all clouds to be thick, single layer clouds. Partly cloudy pixels are treated as the weighted sum of a clear and a cloudy pixel. Pixels that are fully covered with thin clouds are represented by partly cloudy pixels with a thick cloud. Using this cloud model, the AMFs for fully cloudy conditions are determined using the method described in section 3.3. The offline calculated AMFs are stored in a look-up-table. This look-up-table has the same dimensions as listed in Table 3.1, with the difference that the surface pressure is replaced by the cloud pressure and there is a single value of 0.8 used for the albedo of the clouds.

3.4.2 Air Mass Factor for Partly Cloudy Conditions

Partly cloudy pixels are treated as the weighted sum of a clear and a cloudy pixel. In good approximation, the AMF of a partly cloudy pixel is the area and radiance weighted sum of the AMF of a clear and a cloudy pixel:

$$M = w \cdot M_{cloudy} + (1 - w) M_{clear}, \quad [3-9]$$


where w is the weighting factor, M_{cloudy} is the AMF for a cloudy pixel and M_{clear} is the AMF for a clear pixel. The AMFs for clear and cloudy conditions are taken from the look-up-tables described above. The weighting factor w in Eq. [3-9] is the fraction of the photons that originates from the cloudy part of the pixel [Martin *et al.*, 2002] and can be expressed as:

$$w = \frac{f_c \langle I_{cloudy}(p_c) \rangle}{\langle I \rangle}, \quad [3-10]$$

where f_c is the cloud fraction, $\langle I_{cloudy}(p_c) \rangle$ is the average radiance over the fit window for a pixel that is fully covered with a cloud that is located at pressure p_c , and $\langle I \rangle$ is the average measured radiance for the pixel. The cloud weighting factor w is calculated offline as function of Sun/satellite geometry, surface albedo and pressure, and cloud fraction and pressure, and stored in a look-up-table.

3.4.3 Ghost Column

The cloud model treats a cloud as an opaque Lambertian surface of albedo 0.8. The amount of ozone below this surface is called the “ghost column”. It is computed by integrating the ozone profile from the surface to the cloud pressure. The profiles are taken from the Logan, Labow & McPeters climatology. Using the standard deviations provided in this climatology, the ghost column is made a function of the slant column density, in a similar way as the AMF is a function of the slant column density. As is the

	TOGOMI Algorithm Theoretical Basis Document	REF : TOGOMI/KNMI/ATBD/001 ISSUE : 1.2 DATE : 01-11-2003 PAGE : 20
---	--	---

case for the AMF, the ghost column will also be determined by interpolation to the latitude and date of the measurement.

3.4.4 Total Vertical Column Density

For the computation of the total vertical column density, three cases can be distinguished:

- cloud-free pixels
- cloud covered pixel
- partly cloudy pixels.

For a cloud free pixel the total vertical column density N_t is given by:

$$N_t = \frac{N_s}{M_{clear}}, \quad [3-11]$$

where N_s is the slant column density and M_{clear} is the AMF for clear atmosphere.


For a cloudy pixel the total vertical column density is given by:

$$N_t = \frac{N_s}{M_{cloudy}} + N_g, \quad [3-12]$$

where N_g is ghost column density. For a partly cloudy pixel the total vertical column density is given by:

$$N_t = \frac{N_s + w \cdot M_{cloudy} \cdot N_g}{M}, \quad [3-13]$$

where the AMF, M , is determined according to equation [3-9]. For a cloud-free scene, Eq. [3-13] reduces to Eq. [3-11], and for fully cloudy pixels it reduces to Eq. [3-12].

	TOGOMI Algorithm Theoretical Basis Document	REF : TOGOMI/KNMI/ATBD/001 ISSUE : 1.2 DATE : 01-11-2003 PAGE : 21
---	--	---

4. ERROR ANALYSIS

In this section a preliminary error analysis for the TOGOMI total ozone product is presented. This error analysis has originally been done for the OMI ozone DOAS product using simulated spectra [Veeffkind *et al.*, 2001], and has been updated for the GOME instrument. The sensitivity of the product is tested for the following sources of error:

- forward models errors
- a priori errors
- instrument errors.

As already discussed in Chapter 3, there are three main steps in the DOAS algorithm: computation of the slant column density, computation of the AMF, and cloud correction. The sensitivity of these steps to the various errors is very different. Therefore, the error sensitivity of the main steps is treated separately in Sections 4.1, 4.2 and 4.3. All errors are combined in Section 4.4, to obtain the error sensitivity of the end product. Finally, in Section 4.5 we will focus on errors for some exceptional cases, such as desert dust, biomass burning, and polar stratospheric clouds.

4.1 Slant column density

The slant column density fits an analytical function to the measured Sun normalized radiance spectrum. Before applying this fit, the effective spectral resolution of the GOME spectra is reduced by applying a low pass filter and the measured GOME solar irradiance spectrum has to be interpolated to the wavelength grid of the radiance spectra. Besides the GOME spectra, reference spectra of ozone are used in the fit.

4.1.1.1 Forward model errors

The forward model that is used is the analytical function that is fitted to the measured radiance spectrum. The absorption by BrO, SO₂, and NO₂ are ignored in this fit. The effect of neglecting these gases in the slant column density fit was tested by fitting simulated spectra with low and high concentrations of these gases. These test show that the error due to neglecting BrO, SO₂ and NO₂ is generally less than 0.5%, and is mainly caused by variations in BrO and NO₂.

4.1.1.2 A priori errors

The a priori information that is used are reference spectra of the ozone cross section and the Ring effect. The effective spectral resolution of the reference spectra is reduced by applying a low pass filter. Therefore, the effective slit function is known very accurately, as it is determined by the low pass filtering. The ozone cross section is temperature dependent, so an effective temperature of ozone is assumed.



The accuracy of the ozone cross sections is estimated to be $\sim 2\%$ [Bass and Paur, 1986; Orphal, 2002]. Therefore, the error in the slant column density is estimated to be $\sim 2\%$ [Van Roozendaal et al., 2002]. The DOAS technique only uses the spectral features over a fit window, and is thus insensitive to errors in the absolute absorption cross section due to for example offsets.

The temperature dependency of the ozone cross section in the current GOME fit-window (10 nm wide, centered around 330 nm) is about 3%/10 K. Due to the use of an effective ozone cross-section based on ECMWF temperatures (see section 3.2.4), the expected error in the slant column density is estimated to be less than 0.5%. When using the 5 nm wide fit-window centered around 334.1 nm, which is optimized such that the temperature dependence is minimal, the resulting error in the slant column density is expected to be less than 0.3%.


4.1.1.3 Instrument errors

There are different instrument effects that have to be considered:

- radiometric noise
- radiometric additive factor
- radiometric multiplicative factor
- spectral structure
- spectral calibration error
- spectral stability

The radiometric noise of GOME in the 325-340 nm range is better than 1000. For the proposed fit windows the expected error in the slant column density due to radiometric noise is less than 1%. As discussed in Section 3.2.3, a radiometric additive factor (offset) in the radiance measurement that is constant over the entire fit window is accounted for in the DOAS fit function. This is not the case for the solar irradiance measurements, but offsets in the solar irradiance spectrum can easily be corrected for, since the solar irradiance can be measured with a high signal-to-noise and there are several other instruments that can be used for comparison. Hence, the error in the slant column due to additive errors is expected to be negligible. Section 3.2.3 discusses the effect of multiplicative errors (scale factors) that are constant over the fit window. The DOAS fit function can deal with this kind of error, so no effect on the slant column density is expected.

The DOAS method is sensitive to errors in the spectral calibration. The spectral calibration of the GOME level-1 spectra is improved with the GomeCal package, using the Fraunhofer lines in the solar irradiance and Earth radiance spectra, as described in section 3.1. Using this method, the spectral calibration uncertainty is estimated to be less than $1/100^{\text{th}}$ of a pixel, corresponding to about 0.001 nm for the DOAS fitting window. The error in the slant column density due to a spectral calibration error of $1/100^{\text{th}}$ of a pixel is less than 0.5%.

	TOGOMI Algorithm Theoretical Basis Document	REF : TOGOMI/KNMI/ATBD/001 ISSUE : 1.2 DATE : 01-11-2003 PAGE : 23
---	--	---

Due to temperature variations of the GOME instrument, the wavelength grid varies over an orbit. Therefore, the wavelength grid of the earth radiances differs from that of the solar irradiances. The maximum shift between the Earth radiances and solar irradiances (the spectral stability) is less than $1/10^{\text{th}}$ of a pixel. To determine the slant column density, the radiance and irradiance are brought onto the same wavelength grid, which involves interpolation. The effect of spectral stability was tested by shifting the wavelength grid of the solar irradiance, and is estimated to be less than 0.25% for a spectral stability of $1/10^{\text{th}}$ of a pixel.

4.2 Air mass factor (AMF)

The AMF is determined for clear and cloud covered pixels by interpolating in a pre-calculated look-up table, as described in Section 3.3. The following is a summary of errors in computing the AMF.

4.2.1.1 Forward model errors

In the radiative transfer model calculations that are performed to construct the AMF look-up-table, scattering and absorption by aerosol particles is ignored. For boundary layer aerosol, the error in the AMF for normal aerosol loads is estimated to be 0.2%. The effect of absorbing aerosol layers at higher altitude, for example desert dust or smoke layers, is larger. These cases are discussed in Section 4.5.


Clouds are represented in the forward model calculations by Lambert surfaces with an albedo of 0.8. As shown by *Koelemeijer and Stammes* [1999] and *Koelemeijer* [2001], this approximation results in differences of the order of 1% for the AMF for ozone as compared to more sophisticated cloud models. It is clear that this error only occurs when computing the AMF for the cloud covered part of the pixel.

4.2.1.2 *A priori* errors

The a priori information that is used to determine the AMF for the cloud free part of the pixels is the surface reflectivity and the ozone profile. For the cloud covered part of the pixel the cloud pressure and the ozone profile is used.

The sensitivity of the AMF on the ozone profile was estimated from latitudinal and seasonal variations of the AMF as computed for the Logan, Labow & McPeters ozone climatology. Using the relation between the AMF and the slant column density in a similar way as discussed in Section 3.3, the error in the AMF can be estimated. The results show that the sensitivity of the AMF on the ozone profile increases with the geometrical AMF. The maximum error in the AMF due to the ozone profile is estimated as 2%, whereas the average error is estimated to be less than 0.5%.

For the cloud free part of the pixel, the AMF depends on the surface reflectivity. The seasonal variation of the surface reflectivity in the UV is on average 0.03. Assuming that the accuracy of the surface reflectivity is of this order, the resulting error in the AMF is less than 0.3%.

	TOGOMI Algorithm Theoretical Basis Document	REF : TOGOMI/KNMI/ATBD/001 ISSUE : 1.2 DATE : 01-11-2003 PAGE : 24
---	--	---

The sensitivity of the AMF for a cloud covered pixel was estimated from the variations in the AMF as a function of the cloud pressure. For clouds at an altitude of 1 km altitude an error of 100 hPa in the cloud pressure results in a 0.6% error in the AMF. For clouds at 10 km altitude this error has increased to 3%. The average error is estimated as 1%.

For a cloud free pixel, the total error in the AMF is estimated to be 0.6%, for a cloudy pixel the error is estimated to be 1.5%.

4.3 Cloud correction

In the cloud correction step, the amount of ozone below the cloud (ghost column) is calculated using an ozone profile climatology and the cloud pressure. The a priori error in the ozone profile climatology was estimated by looking at the standard deviations at each level, as supplied as part of the climatology. This error in the ghost column is estimated to be 25%. The error in the ghost column due to an error of 100 hPa in the cloud pressure is of the order 4 DU. For typical conditions, the total error in the ghost column is estimated to be 40%.

4.4 Error Budget

The error estimate for the total vertical column density is derived from the error estimates of the slant column density, the AMF, and ghost column. The error in the slant column density is about 2.3%. The expected accuracy of the AMF depends on the cloud fraction. The accuracy of the cloud fraction is expected to be better than 0.1 [*Koelemeijer et al., 2002*]. This results in an error in the AMF of the order 0.8%. The total error in the AMF is 1.0% for a cloud free pixel, for a cloudy pixel this is 1.7%. For a partly cloudy pixel an error of 1.4% is expected.

For a cloud free pixel the vertical column density is computed by dividing the slant column density by the AMF. The total error of the vertical column density for this case is 2.5%. For a cloud covered pixel this error increases to 3.3%, due to the uncertainty in the ghost column. For partly cloudy pixels, the error will be in between the value for the clear and cloudy case, and is estimated to be 2.8%.




TOGOMI
Algorithm Theoretical Basis
Document

REF : TOGOMI/KNMI/ATBD/001
ISSUE : 1.2
DATE : 01-11-2003
PAGE : 25

Table 4.1. Error estimates for the TOGOMI total ozone product.

Source	Total Error [%]	Relative Error [%]
<i>Slant Column Density</i>		
Other trace gases	0.5	
Absorption cross section	2	
Instrument response function	0.1	
Atmospheric temperature	<0.5	<0.5
Instrument signal-to-noise	<1	<1
Instrument spectral calibration	0.5	
Instrument spectral stability	0.25	
<i>Air mass factor</i>		
Aerosols	0.2	0.2
Clouds	1	1
Ozone profile	0.5	0.5
Surface reflectivity	0.3	
Cloud pressure	1	1
Cloud fraction	0.8	0.8
<i>Cloud Correction</i>		
ghost column	40	40
<i>Vertical Column Density</i>		
Clear	2.5	1.2
Partly Cloudy	2.8	1.7
Cloudy	3.3	2.2

For determining trends in ozone, the relative errors are important. The relative errors are defined as errors that can vary for two measurements for the same location for two successive days. This criterion was used to determine which of the errors in Table 4.1 are relative errors. For some error sources, like for example the spectral calibration, it is quite arbitrary to what extent this error of relative nature. For these arbitrary cases, the error was marked to be fully of relative nature, making the budget for relative errors in Table 4.1 a conservative estimate. As can be seen in Table 4.1, the relative error of the vertical column density is 1.2% for a cloud-free pixel, 2.2% for a cloudy pixel and 1.7% for a partly cloudy pixel. Thus, for cloudy conditions, the relative error is dominated by errors related to clouds.

	TOGOMI Algorithm Theoretical Basis Document	REF : TOGOMI/KNMI/ATBD/001 ISSUE : 1.2 DATE : 01-11-2003 PAGE : 26
---	--	---

4.5 Exceptional Cases

In some exceptional cases the error in the ozone column can be considerably larger than the errors in the error budget (Section 4.4). Here, the effect of desert dust aerosols, biomass burning, polar stratospheric clouds, and large solar zenith angles are discussed.

4.5.1.1 Desert Dust

Desert dust can be transported in elevated layers over thousands of kilometers away from the source region. This situation is frequently observed over the equatorial Atlantic during late summer and fall. Scattering and absorption by these desert dust aerosols change the radiative properties of the atmosphere, and thus affect the AMF. To quantify the effect of ignoring these aerosols in the AMF calculations, retrievals were performed on simulated spectra with and without desert dust. Simulated spectra were generated for desert dust layers at 2.5 and 3.5 km altitude. The optical thickness of these layers was 1.0, and the single scattering albedo was 0.8. These calculations show that the effect of ignoring desert dust aerosols yields an underestimation of the ozone vertical column density of 0.4 to 0.8% for the layer at 2.5 km, and 0.9 to 1.4% for the layer at 3.5 km.

4.5.1.2 Biomass Burning

Biomass burning and forest fires are an important source of absorbing aerosols. However, besides increased column amounts of absorbing aerosols, biomass burning also causes increased amounts of tropospheric ozone. Both the presence of absorbing aerosols and the increased tropospheric ozone levels will cause an underestimation of the vertical column density of ozone. To estimate both effects, simulations were performed with biomass burning aerosols and increased ozone concentrations in the lowest three kilometers of the atmosphere. Aerosols with a single scattering albedo of 0.9 and an optical thickness of 1.0 were assumed. Tropospheric ozone levels were increased with 20 DU. These simulations show that each effect causes an underestimation of the ozone vertical column density of about 4%. The combined effect of having both absorbing aerosols and increased ozone levels gives an underestimation of 8-9%.

4.5.1.3 Polar Stratospheric Clouds

The effect of polar stratospheric clouds (PSCs) depends strongly on the optical thickness of the PSC layer and on the PSC layer altitude. Also, the effect increases with increasing solar zenith angle. To quantify the effect of PSCs on the retrieval of the total ozone column, a study was conducted that tested different PSC types at two altitudes [Veeffkind, 2002]. These altitudes were chosen just below and just above the ozone maximum. The results of this study show that for the most frequently observed type of PSCs (Type I), which are characterized by a typical optical thickness of 0.01, the maximum error in the ozone column is less than 3 %. It is noted that approximately 90 % of all PSCs are of Type I. For Type II PSCs, which have a typical optical thickness of 0.04, the maximum error is 11 % and on average the error is less than 0.5 %. The errors are largest for PSCs of Type III, which have a typical optical thickness of 0.4. For this type the error can be as large as 40 %, but on average the error is still below 5 %. Also, it is noted that less than 1 % of all PSCs are of Type III.




4.5.1.4 Large Solar Zenith Angles

Large solar zenith angles ($>80^\circ$) are especially important for observing ozone hole conditions. The error in the ozone vertical column density is larger than for normal geometries due to the following effects:

- Decreased instrument single-to-noise
- Large variations in the ozone profiles
- Large temperature variations
- Decreased sensitivity for tropospheric ozone

Errors in the radiative transfer models due to spherical effects of the atmosphere.

Although none of the effects listed above will dominate, the combination of all these effects will lead to larger errors for high solar zenith angles than for normal Sun/satellite geometries. As a first order estimate, we expect the errors in the ozone vertical column density to increase to 5%. Various GOME and TOMS total ozone studies show that these errors increase with solar zenith angle, and are of the order 5-10% [*Lambert et al.*, 1999, *Van Roozendaal et al.*, 2002].

	TOGOMI Algorithm Theoretical Basis Document	REF : TOGOMI/KNMI/ATBD/001 ISSUE : 1.2 DATE : 01-11-2003 PAGE : 28
---	--	---

5. VALIDATION

The GOME total ozone data generated by the algorithm will be validated against Brewer and Dobson ground-based measurements, GDP V3 ozone columns, and TOMS total ozone, using the set of 2257 GOME orbits that have been used in the GDP 3.0 delta validation campaign [Lambert, 2002]. This selection ensures an analysis of total ozone product quality for a range of observing conditions (solar zenith angle, surface albedo, ozone vertical column, cloud fraction and cloud top height, temperature profile) and atmospheric circumstances (seasonal variations, meridian structure, winter-spring polar photochemistry/ozone depletion and midnight sun). The orbits cover the periods 1996 through 2001 to assess the long-term stability of the product.

The new GOME vertical ozone columns will be compared with the GDP V3 total ozone columns for all data in all orbits. The differences/improvements with respect to the GDP data are studied for each processing step separately (SCD, AMF, cloud information).

A validation exercise will be conducted against co-located ground based measurements of 140 Dobson, Brewer and M-124 ground based stations (<http://lap.physics.auth.gr/o3safval/stationstat.htm>). The results will be thoroughly analyzed, particularly focusing on the solar zenith angle (SZA) and seasonal dependence of the deviations between GOME and station measurement.

Comparison with EP-TOMS total ozone measurements. EPTOMS Level 3 total ozone data is available through (<ftp://jwocky.gsfc.nasa.gov>) on a 1.00 x 1.25 degree grid.. For all GOME ground pixels in the validation set a corresponding TOMS value is derived by nearest-neighbour. The differences will be studied as a function of latitude and season.

Possible unsatisfactory validation results will be traced back to algorithm settings in the GOME processing SW system. If deemed necessary, the GOME ozone column algorithm will be improved.